Astron. Astrophys. 347, 30–36 (1999)

ASTRONOMY AND ASTROPHYSICS

Helical jets in blazars

I. The case of Mkn 501

M. Villata and C.M. Raiteri

Osservatorio Astronomico di Torino, Strada Osservatorio 20, I-10025 Pino Torinese (TO), Italy (villata@to.astro.it)

Received 25 November 1998 / Accepted 27 April 1999

Abstract. Multifrequency observations of the BL Lacertae object Mkn 501 show a peculiar behaviour of its spectral energy distribution (SED): the synchrotron spectrum presents a discontinuity between the radio-to-UV part and the X-ray one; moreover, in 1997 BeppoSAX and RXTE detected an exceptional brightening and hardening of the X-ray spectrum, never seen before in any blazar, whereas the lower-frequency emission did not show any substantial change. Classical one-zone and inhomogeneous-jet synchrotron-emission models do not offer any simple and self-consistent explanation for this kind of behaviour. We present a model of inhomogeneous curved–helical jet that allows to explain both phenomena without invoking intrinsic variations of the emission, but assuming that it remains constant in time. The spectacular brightening in the hard X-ray band is interpreted as due to a variation of the jet orientation, probably caused by the orbital motion of the parent black hole in a binary black hole system (BBHS), and hence to a change of the relativistic beaming factor. The predicted flux variations are more noticeable at the highest synchrotron frequencies, which are emitted from the inner and most inhomogeneous part of the jet. A comparison between the model results and the most recent Space VLBI observations reveals a fair agreement and allows to derive an estimate of the BBHS physical parameters. The results of the present work, together with those of previous studies, support the hypothesis of the existence of BBHSs as central engines of active galactic nuclei (AGNs). Their possible role in the ambit of the unified schemes for AGNs is finally discussed.

Key words: galaxies: BL Lacertae objects: general – galaxies: BL Lacertae objects: individual: Mkn 501 – galaxies: jets – galaxies: nuclei – galaxies: quasars: general

1. Introduction

Misalignments and bendings have been observed in a number of radio (and optical) jets (e.g. Zensus 1997), thus revealing these distortions as a common feature of radio-loud active galactic nuclei (AGNs). Begelman et al. (1980) argued that such a phenomenon can be due to the presence of binary black hole systems (BBHSs) as central engines of the bent jets. Conway & Wrobel (1995; see also Conway & Murphy 1993) analysed VLBA and MERLIN images of Mkn 501 that show a quasi-orthogonal misalignment of the jet occurring very close to the core. In their work they infer that this strong apparent curvature is the result of the projection of a helical pattern, possibly generated by Kelvin–Helmholtz instabilities driven at the origin through orbital motion of the central engine in a BBHS.

Other authors investigated jet helical distortions and related BBHSs (e.g. Roos 1988; Kaastra & Roos 1992; Hardee et al. 1994, 1997; Villata & Ferrari 1995; Appl et al. 1996; Tateyama et al. 1998; Villata et al. 1998). In particular, Villata et al. (1998) showed how the quasi-periodic behaviour of the blazar OJ 287 optical light curve can be explained by the presence of a BBHS and consequent orbital and precession motions of the emitting jets. VLBI observations of this source confirm the existence of a helical path in the radio structure (Vicente et al. 1996).

Jet helical morphologies can thus be the product of orbital and precession motions, the former being probably responsible for small-scale distortions, seldom recognizable with the currently achievable instrumental resolutions, the latter generating larger-scale bendings. Recent Space VLBI maps of Mkn 501 (Giovannini et al. 1998) seem to show two different-scale helical structures superimposed to each other. The larger one is that recognized by Conway & Wrobel (1995) as responsible for the orthogonal misalignment, while the smaller-scale one did not appear in the lower-resolution VLBA images they analysed.

Mkn 501 has recently been the object of intensive multiwavelength campaigns, since it was detected at TeV energies (Quinn et al. 1996; Bradbury et al. 1997; Catanese et al. 1997; Aharonian et al. 1997). One of the most important results of these observations has been the detection of an exceptional brightening and hardening of the X-ray spectrum in April 1997 by BeppoSAX (Pian et al. 1998; see also Ghisellini 1998).

As suggested by Villata et al. (1998), strong brightness and spectral changes in blazars could be due to orientation changes of the emitting jet rather than to, as currently believed, intrinsic variations of the power output. In the present paper we investigate this possibility for the case of the observed X-ray variations of Mkn 501: the emitting relativistic jet is modelled as a curved jet suffering orientation variations, as expected in the case of an orbiting jet in a BBHS. The different states of the radio-to-X-

Send offprint requests to: M. Villata

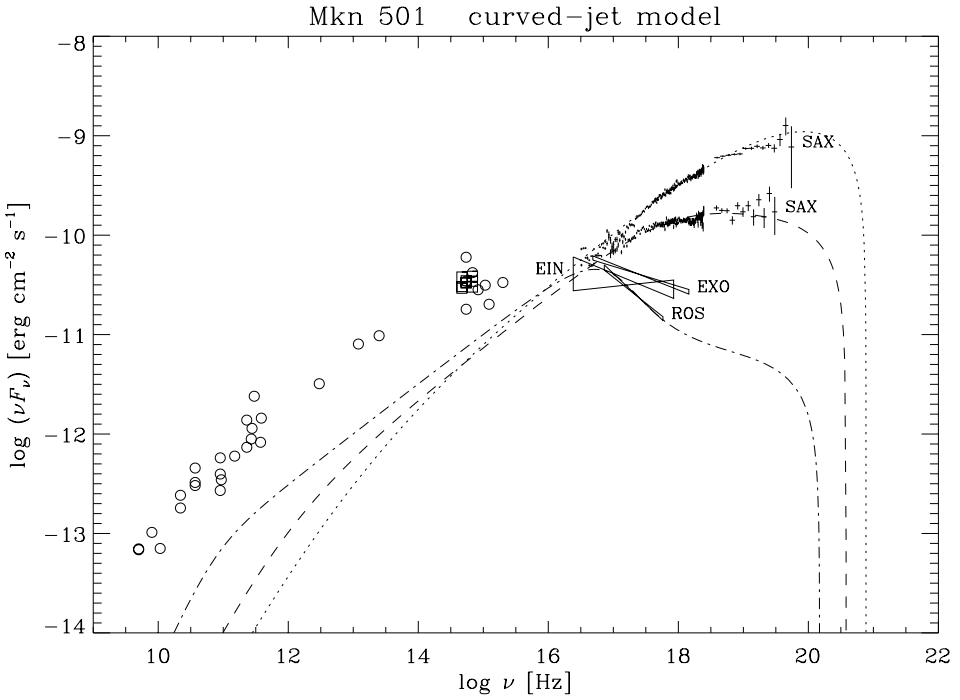

Fig. 1. The observed SEDs of Mkn 501; the curves indicate curved-jet model fits to the X-ray SEDs observed in different brightness states; the model results are obtained by small orientation changes (a few degrees) of a curved jet emitting a steady synchrotron flux

ray spectral energy distribution (SED) of Mkn 501 (see Sect. 2) are fitted by means of synchrotron emission models in inhomogeneous curved/helical jets, maintaining a steady intrinsic synchrotron flux and allowing for small displacements of the jet with respect to the line of sight (Sect. 3).

The second goal of this work is to find possible correlations between the results of the steadily-emitting curved-jet model and the most recent Space VLBI radio maps (Sect. 4). A conclusive discussion will be performed in Sect. 5.

2. The observational background

Fig. 1 shows the observed synchrotron SEDs of Mkn 501 (data from Pian et al. 1998): satellite X-ray data from Einstein, EXOSAT, ROSAT, and BeppoSAX are labelled; circles refer to lower-frequency literature data. Squares represent the optical data taken by the Torino monitoring group simultaneously with the BeppoSAX pointings of April 1997. The observations were done with the $1.05\,\mathrm{m}$ REOSC telescope of the Torino Astronomical Observatory with a 1242×1152 pixel CCD camera in the Johnson's BV and Cousins' R bands. These data fall in the range of the previous optical data, indicating that the optical flux was not affected by the outburst in the X-ray band.

From Fig. 1 one can notice the extraordinary X-ray brightness levels detected by BeppoSAX in April 1997 (Pian et al. 1998). The exceptionality of this discovery resides not only in the brightness and hardness of the X-ray spectrum, never detected before in any blazar, but also in the strong "break" in the SED between the X-ray band and the lower frequencies, which is firmly stated by the presence of simultaneous optical data. An even more abrupt discontinuity between the optical and X-ray bands appears from the preliminary BeppoSAX data published by Pian et al. (1999), referring to observations done in April–May 1998. Moreover, a similar break has been recently discovered also in PKS 2155−304, again by BeppoSAX (Chiappetti et al. 1999).

Classical homogeneous and inhomogeneous models for the description of the synchrotron emission do not explain such a concavity in the spectral shape. A possible explanation of the SED behaviour can be found in the curvature of the synchrotron-emitting jet. Indeed, a curved inhomogeneous relativistic jet emitting different frequencies at different distances from its apex would appear to have more or less flux at a given frequency according to the orientation of the jet segments that contribute to it with respect to the line of sight, because of relativistic beaming. Thus, peaks (hollows) in the SED of a source would correspond to emitting portions of the jet more (less) collimated with the observer's direction. In the case of Mkn 501, the "missing" flux at soft X-ray energies would be the effect of a larger viewing angle of the corresponding jet emitting segment.

Moreover, the same jet would appear to have different SED shapes along different lines of sight, and even the distinction between radio and X-ray selected (or between LBLs and HBLs; e.g. Padovani & Giommi 1995) sources might be explained by this line-of-sight dependence. Vice versa, in the case that the bent jet changes its orientation and shape, as expected in the presence of a BBHS, even the same observer could notice strong changes in the spectral shape, like those observed in Mkn 501, without the need of intrinsic flux variations. In the same way, this scenario could also explain another peculiarity of the Mkn 501 X-ray spectrum reported by Lamer & Wagner (1998): the anti-correlation between the total flux and the spectral hardness shown by the RXTE observations of July 1997, an opposite behaviour with respect to that observed by BeppoSAX three months before.

3. The model

Orbital and precession motions can generate jet bendings through different processes, according to the physical properties of the jet. A ballistic treatment is suitable for a "heavy" (much denser than the surrounding medium) jet (e.g. Blandford & Icke 1978; Lupton & Gott 1982; Jägers & de Grijp 1985; Kaastra & Roos 1992), whereas a "lighter" jet should be treated hydrodynamically, by an analysis of the linearized time-dependent fluid equations and by hydrodynamical simulations (e.g. Hardee & Norman 1988; Birkinshaw 1991; Hardee et al. 1994, 1997). In any case, the jet response to the perturbing binary motions is some kind of helical structure. A reliable and complete treatment of such a complex problem should take the magnetic field dynamics into account, but a complete magnetohydrodynamic treatment has not been attempted yet.

The main aim of the present work is to show the consequences of the jet bending on the observable quantities, independently of how the bending has been produced. In general and for simplicity, we consider that a relative motion between the parent black hole (possibly in a BBHS) and the ambient medium exists, so that we expect some sort of curvature to be generated along the jet, of hydrodynamic or magnetic origin, or both.

We investigate two different kinds of curvature: a simple 2-D monotonic curvature (like that generated by rectilinear relative motion) and a more complex helical shape (as the consequence of orbital motion).

3.1. Curved jet

We first consider an inhomogeneous jet with a simple monotonic 2-D curvature. The jet axis lies in the positive x–z plane and it is tangent to the z-axis at $x = z = 0$, which we identify as the origin of the jet, i.e. where the jet starts to emit the highest synchrotron frequencies. The jet axis is described by the curve

$$x = az^b\,, \quad a > 0\,, \quad b > 1\,; \tag{1}$$

$$\zeta(z) = \arctan\frac{\mathrm{d}x}{\mathrm{d}z} = \arctan\left(abz^{b-1}\right) \tag{2}$$

is the angle between the jet axis and the z-axis, and

$$l(z) = \int_0^z \sqrt{1 + a^2b^2w^{2(b-1)}}\,\mathrm{d}w \tag{3}$$

is the length of the jet axis.

In the following we are interested in small viewing angles (with respect to the z-axis and the first portion of the jet), so that we can truncate the jet when $\zeta = 45^\circ$ with negligible error. Being x, z, and l non-dimensional quantities, for simplicity we fix this to occur at $z = 1$, so that, from Eq. (2), $ab = 1$.

The jet shape described above must be intended as that seen by the observer, taking the different light travel times into account, as well as possible plasma velocity components deriving from motion of the curved path. In other words, the above jet axis must be intended as the curve tangent to the emitting-plasma velocity vectors as they were when the observed radiation started, at different times along the jet.

The inhomogeneity of the jet is similar to that of the models by Ghisellini & Maraschi (1989; see also Ghisellini et al. 1985; Maraschi et al. 1992). We assume that each slice of the jet emits, in the plasma rest reference frame (primed frequencies refer to this frame), a range of frequencies between $\nu'_{\min}$ and $\nu'_{\max}$ that are supposed to be decreasing with increasing l:

$$\nu'_{\min}(l) = \nu'_{\min}(0)\left(1 + \frac{l}{l_1}\right)^{-c_1}\,, \quad c_1 > 0\,, \tag{4}$$

$$\nu'_{\max}(l) = \nu'_{\max}(0)\left(1 + \frac{l}{l_2}\right)^{-c_2}\,, \quad c_2 > 0\,, \tag{5}$$

where $\nu'_{\min}(0)$ and $\nu'_{\max}(0)$ are the values at $l = z = 0$, l_1 and l_2 are length scales. In the following we assume that $\nu'_{\min}(0) = \nu'_{\max}(0) = \nu'_0$.

The observed flux density at frequency ν is assumed to be (see e.g. Begelman et al. 1984; Urry & Padovani 1995)

$$F_\nu(\nu) \propto \delta^3\nu^{-\alpha_0}\,, \tag{6}$$

where α_0 is the power-law index of the local synchrotron spectrum (which we fix to be $\alpha_0 = 0.5$) and

$$\delta = [\gamma(1 - \beta\cos\theta)]^{-1} \tag{7}$$

is the beaming or Doppler factor, β being the bulk velocity of the emitting plasma in units of the speed of light, $\gamma = (1-\beta^2)^{-1/2}$ the corresponding Lorentz factor, and θ the angle between the velocity vector and the line of sight. In our curved-jet model θ (and hence δ) varies along the jet:

$$\cos\theta(l) = \cos\psi\cos\zeta(l) + \cos\phi\sin\psi\sin\zeta(l)\,, \tag{8}$$

where ψ is the angle between the z-axis and the line of sight, and ϕ its azimuthal angle starting from the x-axis.

Moreover, we introduce an intrinsic flux-density dependence on l, so that the observed flux density at frequency ν coming from a jet slice of thickness $\mathrm{d}l$ can be expressed as

$$\mathrm{d}F_\nu(\nu) \propto \left(1 + \frac{l}{l_0}\right)^{-c_0}\delta^3(l)\nu^{-\alpha_0}\,\mathrm{d}l\,, \quad c_0 \geq 0\,. \tag{9}$$

The total flux density at frequency ν coming from the whole jet is obtained by integrating along all the portions that contribute to that observed frequency:

$$F_\nu(\nu) \propto \nu^{-\alpha_0}\sum_i \int_{\Delta z_i(\nu)} \left[1 + \frac{l(z)}{l_0}\right]^{-c_0}\delta^3(z)\frac{\mathrm{d}l}{\mathrm{d}z}\,\mathrm{d}z\,, \tag{10}$$

where $\Delta z_i(\nu)$ are the z intervals corresponding to the jet segments emitting the observed frequency ν along the line of sight, i.e. where the condition

$$\delta(z)\nu'_{\min}(z) \leq \nu \leq \delta(z)\nu'_{\max}(z) \tag{11}$$

is verified.

The proportionality constant in Eq. (10) is considered independent of time, i.e. *intrinsic variations of the flux are not allowed*.

Fig. 1 shows three model fits to the Mkn 501 SEDs obtained by taking the X-ray data (BeppoSAX and ROSAT) only into account. The relevant model parameters, equal for the three curves, are: $a = 1/2$, $b = 2$, $\log l_1 = -3.2$, $\log l_2 = -1.6$, $c_1 = c_2 = 4$, $\log \nu'_0 = 19.6$, $\alpha_0 = 0.5$, $\gamma = 10$, $c_0 = 0$. The fit to the brightest BeppoSAX state has been obtained with $\psi = 1°$ and $\phi = 140°$. The lower one has $\psi = 6°$ and $\phi = 50°$; whereas the X-ray state detected by ROSAT is fitted by $\psi = 12°$ and $\phi = 22°$. Thus, all the three very different X-ray spectral shapes are well fitted by the same steady intrinsic emission of the same curved jet, the difference depending on the jet orientation only. As expected, being higher frequencies emitted closer to the origin, the hardest and brightest state corresponds to a very small viewing angle with respect to the z-axis, i.e. the first and hardest-emitting portion of the jet is almost aligned with the line of sight. As the orientation changes and softer-emitting parts present the smallest viewing angles, the X-ray spectrum becomes fainter and softer, whereas some brightening of the lower-frequency emission is obtained.

However, as in the case of the classical one-zone and inhomogeneous-jet models, the present curved-jet model cannot explain the X-ray and the radio-to-UV spectra simultaneously, being the latter much brighter than the model predictions. Indeed, the optical data contemporaneous to the BeppoSAX pointings pose severe constraints to the model. A different kind of curvature is needed.

3.2. Helical jet

Since the above curvature model describes the X-ray part of the Mkn 501 SEDs very well, we maintain this model for the first portion of the jet, and extend its path by twisting it in a helical shape with a similar curvature.

The pitch angle of the helix is fixed to be $\zeta_{\rm h} = 30°$ and the line of sight forms an angle $\psi_{\rm h} = 25°$ with the helix axis, so that the viewing angle of the helical path reaches a minimum $\theta_{\rm h,min} = 5°$ at each turn of the helix, and the frequencies there emitted will be the most beamed and will produce peaks in the SED. This minimum viewing angle, more or less, corresponds to the above fitting values of the angles ψ and ϕ, once (a given portion of) the above curved-jet is inserted into the helical pattern, as a tangent prolongation of it and with the concavity towards the helix axis. Hence, the orientation changes of the curved–helical jet can be seen as a rotation of the helical structure around its axis, with the first curved portion slightly deviating from the helical pattern. In particular, the small displacement of about $6°$ between the two BeppoSAX states would correspond to a rotation of about $1/60$ of a complete orbit. Comparing this with the 9-day time elapsed between the two observations, one can extrapolate an orbital period of about $1.5\,{\rm yr}$ (cf. Sect. 4).

We assume that the curved model covers an angle of $30°$, i.e. the jet becomes exactly helical (maintaining a similar curvature) when $\zeta = 30°$. At this point the jet will have $\nu'_{\rm min}$ and $\nu'_{\rm max}$ fixed by Eqs. (2)–(5), namely, with the parameters adopted in Sect. 3.1, $\log \nu'_{\rm min} \approx 7.66$ and $\log \nu'_{\rm max} \approx 13.99$. Moreover, we assume that these values remain constant along the following helical path and also that, as in the curved-jet model, $c_0 = 0$ in Eqs. (9) and (10); the proportionality constant in these equations and the other physical parameters are taken equal to those of the curved model. The last free parameter is the "length" of the helical part of the jet, expressed in terms of the azimuthal angle

$$\varphi = a_{\rm h} z_{\rm h} \tag{12}$$

covered by the helical path, $a_{\rm h}$ being a constant (in our case $a_{\rm h} \approx 57°$) and $z_{\rm h}$ the coordinate along the helix axis.

The formulae relevant to the helical model are similar, mutatis mutandis, to those of the curved-jet model. In particular, the z-axis tangent to the curved jet at the origin is replaced by the $z_{\rm h}$-axis of the helix, so that the length of the helical jet is

$$l_{\rm h}(z_{\rm h}) = \frac{z_{\rm h}}{\cos\zeta_{\rm h}} \tag{13}$$

and its viewing angle at $z_{\rm h}$ is

$$\cos\theta_{\rm h}(z_{\rm h}) = \cos\psi_{\rm h}\cos\zeta_{\rm h} + \sin\psi_{\rm h}\sin\zeta_{\rm h}\cos(\phi_{\rm h} - a_{\rm h} z_{\rm h})\,, \tag{14}$$

where $\phi_{\rm h}$ is the azimuthal difference between the line of sight and the initial direction of the helix. As already seen above, $\theta_{\rm h}$ has a minimum when $\phi_{\rm h} - a_{\rm h} z_{\rm h}$ is zero or a multiple of $360°$, so that the frequencies emitted from the corresponding jet segments will produce peaks in the observed SED. In the case of Mkn 501 we have supposed that the helical part of the jet is homogeneous, in particular that it emits the same frequencies ($7.66 \lesssim \log\nu' \lesssim 13.99$) along the helical path: a single peak close to $\delta(\theta_{\rm h,min})\nu'_{\rm max} \approx 10^{15}$ is then expected. Moreover, if $\varphi_{\rm max}$ is a multiple of $360°$, i.e. the homogeneous jet turns around the $z_{\rm h}$-axis an integer number of times (or a large number of times), its observed SED is independent of $\phi_{\rm h}$, namely of its rotation around the helix axis, because of the exact periodicity. In any case, the above assumptions of homogeneity lead to a fairly stable radio-to-UV spectrum, while the inhomogeneity of the harder-emitting first part of the jet is responsible for the spectacular variations of the X-ray spectral distribution.

In Fig. 2 we show the results of the curved–helical model with $\varphi_{\rm max} = 720°$. The X-ray spectra are the same as in the curved model, since frequencies $\gtrsim 10^{15}$ come from the curved part. The lower-frequency emission comes instead mainly from the helical part, where it is independent of the rotation of the helix, so that the small differences among the three states derive from the different orientation of the curved part.

Thus, this helical prolongation of the curved jet accounts for the radio-to-UV spectral distribution and for its steadiness too. The presence of some variations in the literature data, especially at the lowest frequencies, could be due to a slight inhomogeneity in the rotating jet or, simply, to intrinsic short-term variations. The discordant points in the optical are probably due to the difficulty of separating the optical contribution of the blazar from that of the bright host galaxy.

At this point one might wonder whether some other solution, possibly simpler, can account for the data as well, and, in particular, if the discontinuities in geometry and homogeneity are strictly necessary to explain the data. A simpler model could consist in a "perfect" helix with a single inhomogeneity law.

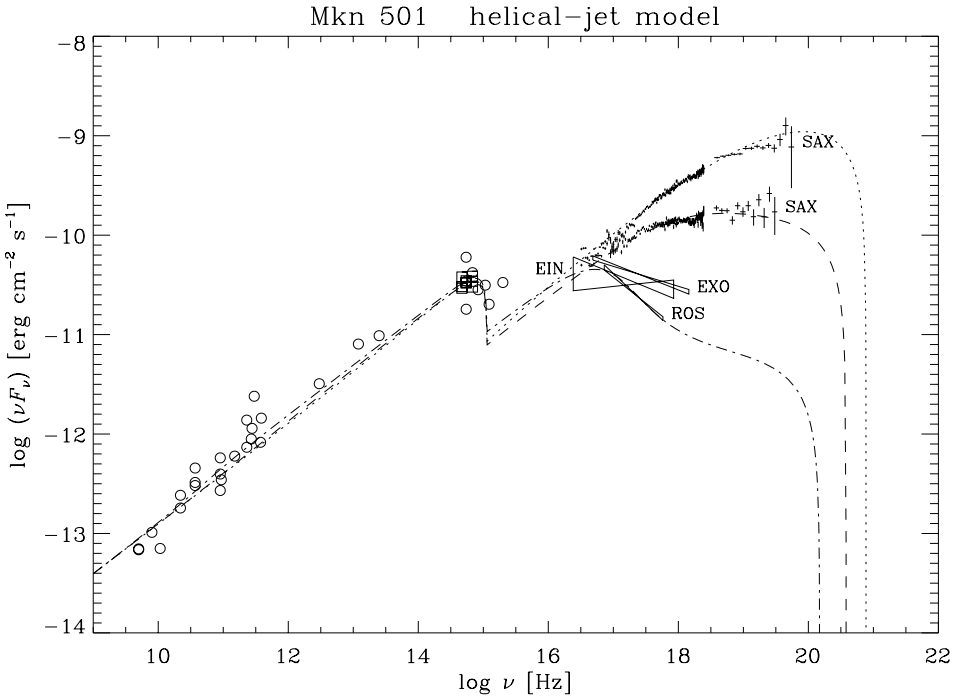

Fig. 2. Helical-jet model fits to the SEDs observed in different X-ray brightness states of Mkn 501; the model results are obtained by small orientation changes (a few degrees) of a curved–helical jet emitting a steady synchrotron flux

Even if the main features of such a solution would not be very different from the adopted one, it does not fit the data as well. However, the supposed deviations are slight: the assumption of homogeneity starts when the inhomogeneity law has reached a quasi-constant trend.

4. Comparison with Space VLBI observations

Space VLBI observations at $18\,\mathrm{cm}$ of Mkn 501 have been presented by Giovannini et al. (1998). Thanks to the high resolution of these new data the structure of the inner and brightest part of the radio jet (a few parsecs) has been partially resolved, while previous ground-based VLBI detections (see e.g. Conway & Wrobel 1995) gave no information at this level. It is now clear that the inner structure is "knotty" with 3–4 (depending on the observation epoch) quasi-equidistant peaks with slightly decreasing intensity. After these bright peaks the luminosity drops dramatically, so that almost all the radio emission comes from them.

In general, we can interpret jet knots as the locations where the jet helical pattern presents the minimum viewing angle, since there the emission is more beamed towards the observer. In our case 3–4 emission knots (probably composed by the actual core plus 2–3 equidistant components of similar brightness) seem to agree well with our helical model where the mathematical choice of $\varphi_{\max} = 720°$ implies 2–3 radio peaks. This agreement on the number of peaks is very surprising and, on one hand, strongly supports the model, on the other hand suggests that we could be not so far from the resolution needed to see the actual helical structure of the jet.

In this scenario a possible proper motion of the radio components should be intended as due to the rotation of the helical path as a consequence of the black hole orbital motion. From a comparison between the two Space VLBI observations (August 1997 and April 1998) Giovannini et al. (1998) estimated an apparent velocity of the central component of about $6.7\,c$ ($H_0 = 50\,\mathrm{km\,s^{-1}\,Mpc^{-1}}$), since they found a displacement of about $1.5\,\mathrm{mas}$ between the two epochs (8 months). Taking the large uncertainties into account, we can estimate that the time needed to cover the distance between two components should be in the range 1–$4\,\mathrm{yr}$, which should correspond to the black hole orbital period. It would not be so far from the 11-year orbital period of the blazar OJ 287 deduced from its optical light curve (Villata et al. 1998). On the other hand, if the radio peaks were the signature of a double helix (of the kind of that observed in M 87; Villata & Ferrari 1995) composed by two stranding jets originating from the two black holes as in the model by Villata et al. (1998), the orbital period would be double: 2–$8\,\mathrm{yr}$. In this case the limb brightening occurring at about $8\,\mathrm{mas}$ from the core and characterizing the radio structure from there outwards could be due to the separation of the two helical components. This different scenario would not change much the results obtained in Sect. 3.

Another interesting feature of the radio maps is that in the first-epoch observations (close to the X-ray brightening of the source), i.e. when the first resolved component is closer to the core, the core itself is more peaked than in the second epoch, when instead it appears elongated towards the departing component, thus suggesting that a new component is coming out and that in 1997 this component was superimposed to the core. According to our model, this would mean that at that time we were seeing the first part of the jet at a small viewing angle, in agreement with the high X-ray state observed in that period (Lamer & Wagner 1998; Ghisellini 1998). On the other hand,

the evidence of a new component in the April 1998 image is in agreement with the lower X-ray flux detected contemporaneously by BeppoSAX (Pian et al. 1999).

From an inspection of the 1991 VLBA images Conway & Wrobel (1995) found a larger-scale periodicity interpreted as the projection of a helical pattern. A comparison with the VLBI map by Giovannini et al. (1998) shows that some features are recognizable in both images. In particular, feature D of Conway & Wrobel (1995) can be identified at the same distance (100–$110\,\mathrm{mas}$) from the core in both maps, with no measurable proper motion. We can interpret the large-scale helical pattern found by Conway & Wrobel (1995) as due to the precession motion of the black hole spin axis, and not to the orbital motion as they suggested, since the signature of this latter can now be seen on smaller scales thanks to the higher resolution of the Space VLBI images.

Because of its short orbital period, the BBHS in Mkn 501 should be a close binary, with a separation of the order of that for which gravitational radiation becomes dominant in the binary orbital evolution, hence we would be in the presence of a BBHS towards the end of its evolution. According to Begelman et al. (1980) the mass of the primary black hole (M) can be deduced from the orbital period (T) for any given value of the mass ratio (M/m) between the primary and secondary components: $M \sim T_{\mathrm{yr}}^{8/5}(M/m)^{3/5}\,10^6\,M_\odot$. Thus, for periods of 1–10 yr and mass ratios in the range 1–100, we can have primary black hole masses from $\sim 10^6$ to $\sim 6\,10^8\,M_\odot$. Accordingly the binary separation would be in the range $5\,10^{-4}-2\,10^{-2}\,\mathrm{pc}$, and the precessional period of the primary could vary from $6\,10^3$ to $4\,10^5\,\mathrm{yr}$, which agrees with the driving frequencies found by Conway & Wrobel (1995). If the jet is emitted from the primary, then the jet orbital radius is $m/(M+m)$ times the above binary separations, thus it would be much smaller than the parsec-scale on which we observe the helical structure. This would mean that the jet must deviate from the helical pattern towards its apex, in agreement with the different curvature we supposed for the initial emitting part of the jet in Sect. 3, and also with the geometry proposed by Conway & Wrobel (1995). The orbital velocity of the primary black hole would be of the order of 10^2–$10^3\,\mathrm{km\,s^{-1}}$.

5. Discussion and conclusions

Different kinds of observational data (Space VLBI radio imaging and spectral energy distribution from the radio to the hard X-ray band) seem to converge in suggesting that the emission of the BL Lacertae object Mkn 501 comes from a curved inhomogeneous jet twisting in a helical shape. Such a model can explain the peculiar double-peaked spectral shape observed during the X-ray brightening as the consequence of the different beaming factor pertaining to different portions of the jet and hence to different emitted frequencies. The spectacular activity recently observed at X-ray energies and the contemporary steadiness of the lower-frequency emission can be explained in terms of small variations of the jet orientation, without resorting to strong intrinsic flux variations in delimited spectral bands.

Both the helical shape and its orientation changes would be generated by the orbital motion of the parent black hole as a component of a BBHS. Very recent Space VLBI images seem to strictly confirm this scenario, showing the "knotty" signature of the helical pattern inside the inner and brightest part of the radio jet, with the same number of peaks predicted by the model fitting the multiwavelength data. Moreover, from a comparison between the Space VLBI data taken at two different epochs one can derive an orbital period of a few years.

In general, a signature of the orbital period should be evident in the light curves, especially at the highest synchrotron frequencies, since they are emitted from the inner, most inhomogeneous part of the jet. In the case of Mkn 501 this happens in the X-ray band and a well sampled X-ray light curve should confirm this picture. Other blazars present periodicity in their historical optical light curves: PKS 0735+17 (Fan et al. 1997), OJ 287 (Sillanpää et al. 1996a, 1996b), ON 231 (Liu et al. 1995; Tosti et al. 1998), 3C 345 (Webb et al. 1988), BL Lacertae (Fan et al. 1998). In the case of OJ 287 Villata et al. (1998) have shown that its optical behaviour is well explained in terms of a BBHS with an orbital period similar to that inferred from the light curve. It is interesting to notice that most of the above objects (3C 345, OJ 287, BL Lacertae, PKS 0735+17) also present helical trajectories of their VLBI radio components (Hardee 1987; Vicente et al. 1996; Tateyama et al. 1998; Gómez et al. 1999).

The steady-emission models discussed in the present paper and in Villata et al. (1998) can explain the observed long-term flux variations, not those occurring on time scales much shorter than the orbital periods. This kind of variability is generally believed to be due to intrinsic flux variations or, as in the model by Camenzind & Krockenberger (1992; see also Schramm et al. 1993; Wagner et al. 1995; Steffen et al. 1995), to a Doppler factor variation (of geometrical origin) of an emitting plasma bubble. In order to obtain short-term variations in the framework of the steady-emission models one could assume the existence of a fine helical structure superimposed to that created by the orbital motion (which in turn is superimposed to that due to the precession motion). Such a fine helical structure might originate from a small misalignment of the jet axis with respect to the black hole spin axis: in this case the flux variations would have time scales of the order of the spin period.

The existence of BBHSs is now supported by an increasing number of observations. One can thus wonder whether they play a major role in explaining the differences observed between the two classes of AGNs belonging to the blazar family: the BL Lac objects and the flat-spectrum radio quasars (FSRQs), and hence between their unified-scheme counterparts: the FRI and FRII radio galaxies (see e.g. Urry & Padovani 1995). Indeed, BL Lacs (and FRIs) are better BBHS candidates in that:

- periodicity in the optical light curve has been recognized mainly for BL Lacs; in any case, they are the most variable objects;
- the FRI jets are more "knotty", which is a sign of a helical pattern, possibly involving a double helix (Villata & Ferrari 1995; Villata et al. 1998); moreover, they are more diffuse

and disturbed; on the other hand BL Lac jets show systematically stronger misalignments than quasars (e.g. Pearson & Readhead 1988; Wehrle et al. 1992; Appl et al. 1996);
– in both BL Lacs and FRIs the direction of the magnetic field is preferentially perpendicular to the jet one (e.g. Gabuzda et al. 1992): one can say that what we see is the projection of a magnetic field that follows the helical path and that becomes evident where the helix points towards us;
– both of them seem to prefer giant host galaxies inside rich clusters, where the probability of galaxy merging and hence of BBHS formation is greater.

Another intriguing conjecture is that all blazars (and all radio-loud AGNs) owe their origin to the presence of BBHSs. In this case the differences between FSRQs and BL Lacs could be interpreted in evolutionary terms: FSRQs (and FRIIs) would represent earlier stages characterized by wide BBHSs with long orbital and precessional periods, whose effects would be less evident and recognizable on our observing time scales and in the radio morphologies. BL Lacs (and FRIs) would occur in more advanced phases, when the system has become a close binary with shorter orbital period, and less power is emitted because of the decreased mass accretion rate onto the central engine, and/or, if the jet is powered by the binary orbital energy, because of its dissipation in the previous stages.

Finally, the BBHS scenario could also enlighten the problem of the difference between radio-loud and radio-quiet AGNs. Wilson & Colbert (1995) suggested that this difference may be associated with the spin of the black hole, considered as the energy source of the radio jets: radio-quiet AGNs, residing in spiral galaxies, would have slowly spinning or non-rotating black holes, while radio-loud AGNs, hosted in merger-generated elliptical galaxies, would have rapidly spinning black holes as the result of the coalescence of the two parent black holes. The present work suggests that the BBHS gives rise to the radio-loud AGN before its coalescence, and that the different amount of energy available in radio-quiet sources, FRI–BL Lacs, and FRII–FSRQs correspond to the different rotational energies of a single black hole, a close binary, and a wide binary, respectively.

Acknowledgements. We wish to thank Elena Pian for providing the multifrequency tabular data of the Mkn 501 SED, and Gabriele Giovannini for useful discussions and anticipation of not yet published Space VLBI data.

References

Aharonian F., Akhperjanian A.G., Barrio J.A., et al., 1997, A&A 327, L5
Appl S., Sol H., Vicente L., 1996, A&A 310, 419
Begelman M.C., Blandford R.D., Rees M.J., 1980, Nat 287, 307
Begelman M.C., Blandford R.D., Rees M.J., 1984, Rev. Mod. Phys. 56, 255
Birkinshaw M., 1991, MNRAS 252, 505
Blandford R.D., Icke V., 1978, MNRAS 185, 527
Bradbury S.M., Deckers T., Petry D., et al., 1997, A&A 320, L5
Camenzind M., Krockenberger M., 1992, A&A 255, 59
Catanese M., Bradbury S.M., Breslin A.C., et al., 1997, ApJ 487, L143
Chiappetti L., Maraschi L., Tavecchio F., et al., 1999, ApJ, submitted
Conway J.E., Murphy D.W., 1993, ApJ 411, 89
Conway J.E., Wrobel J.M., 1995, ApJ 439, 98
Fan J.H., Xie G.Z., Lin R.G., et al., 1997, A&AS 125, 525
Fan J.H., Xie G.Z., Pecontal E., Pecontal A., Copin Y., 1998, ApJ 507, 173
Gabuzda D.C., Cawthorne T.V., Roberts D.H., Wardle J.F.C., 1992, ApJ 388, 40
Ghisellini G., 1998, In: Scarsi L., Bradt H., Giommi P., Fiore F. (eds.) The Active X-Ray Sky. Nucl. Phys. B (Proc. Suppl.) 69, 397
Ghisellini G., Maraschi L., 1989, ApJ 340, 181
Ghisellini G., Maraschi L., Treves A., 1985, A&A 146, 204
Giovannini G., Cotton W.D., Feretti L., Lara L., Venturi T., 1998, In: Proc. 32nd COSPAR Scientific Assembly. Adv. Space Res., in press
Gómez J.-L., Marscher A.P., Alberdi A., Gabuzda D.C., 1999, ApJ, in press
Hardee P.E., 1987, ApJ 318, 78
Hardee P.E., Norman M.L., 1988, ApJ 334, 70
Hardee P.E., Cooper M.A., Clarke D.A., 1994, ApJ 424, 126
Hardee P.E., Clarke D.A., Rosen A., 1997, ApJ 485, 533
Jägers W.J., de Grijp M.H.K., 1985, A&A 143, 176
Kaastra J.S., Roos N., 1992, A&A 254, 96
Lamer G., Wagner S.J., 1998, A&A 331, L13
Liu F.K., Xie G.Z., Bai J.M., 1995, A&A 295, 1
Lupton R.H., Gott J.R., 1982, ApJ 255, 408
Maraschi L., Ghisellini G., Celotti A., 1992, ApJ 397, L5
Padovani P., Giommi P., 1995, ApJ 444, 567
Pearson T.J., Readhead A.C.S., 1988, ApJ 328, 114
Pian E., Vacanti G., Tagliaferri G., et al., 1998, ApJ 492, L17
Pian E., Palazzi E., Chiappetti L., et al., 1999, PASPC, in press
Quinn J., Akerlof C.W., Biller S., et al., 1996, ApJ 456, L83
Roos N., 1988, ApJ 334, 95
Schramm K.-J., Borgeest U., Camenzind M., et al., 1993, A&A 278, 391
Sillanpää A., Takalo L.O., Pursimo T., et al., 1996a, A&A 305, L17
Sillanpää A., Takalo L.O., Pursimo T., et al., 1996b, A&A 315, L13
Steffen W., Zensus J.A., Krichbaum T.P., Witzel A., Qian S.J., 1995, A&A 302, 335
Tateyama C.E., Kingham K.A., Kaufmann P., et al., 1998, ApJ 500, 810
Tosti G., Fiorucci M., Luciani M., et al., 1998, A&AS 130, 109
Urry C.M., Padovani P., 1995, PASP 107, 803
Vicente L., Charlot P., Sol H., 1996, A&A 312, 727
Villata M., Ferrari A., 1995, A&A 293, 626
Villata M., Raiteri C.M., Sillanpää A., Takalo L.O., 1998, MNRAS 293, L13
Wagner S.J., Camenzind M., Dreissigacker O., et al., 1995, A&A 298, 688
Webb J.R., Smith A.G., Leacock R.J., et al., 1988, AJ 95, 374
Wehrle A.E., Cohen M.H., Unwin S.C., et al., 1992, ApJ 391, 589
Wilson A.S., Colbert E.J.M., 1995, ApJ 438, 62
Zensus J.A., 1997, ARA&A 35, 607